Article:
Liu, H, Chu, F, Zhang, J et al. (1 more author) (2020) Nanodroplets impact on surfaces decorated with ridges. Physical Review Fluids, 5 (7). 074201. ISSN 2469-990X

https://doi.org/10.1103/physrevfluids.5.074201

Nanodroplets Impact on Surfaces Decorated with Ridges

Hanyi Liu[1], Fuqiang Chu[1], Jun Zhang[1], Dongsheng Wen[1,2]

[1]*School of Aeronautic Science and Engineering, Beihang University, Beijing 100191, China*

[2]*School of Chemical Process and Engineering, University of Leeds, Leeds, LS2 9JT, UK*

Abstract

The dynamics of droplet impacting on solid surfaces are directly related to a variety of engineering applications. As some industrial processes have been refined to the nano scale, research interest in nanodroplets impact is growing. In this work, molecular dynamics (MD) is employed to investigate the impact of nanodroplets on superhydrophobic surfaces decorated with nanoridges. We confirm that the decorated nanoridges can significantly promote the bouncing performance of nanodroplets, including enlarging the bounce domain, reducing the contact time, and enhancing the bouncing height. We further find that there are five different bounce modes emerging orderly as the dimensionless impact velocity increases, and the variation laws of droplet contact time as well as the bouncing height are closely related to the bounce modes. Our simulation results demonstrate that the velocity restitution coefficient can be fitted as a power function of the dimensionless impact velocity, regardless of the characteristics of nanodroplets and nanoridges. This work elucidates the bounce mechanism for nanodroplets impacting on nanoridged superhydrophobic surfaces, which is of high importance in designing nanostructured surfaces for related applications.

Keyword: Nanodroplet, Molecular Dynamics, Nanostructured Surface, Superhydrophobic, Impact

Introduction

Droplet impacting on solid surfaces is ubiquitous in nature, and it has a wide range of engineering applications, such as ink-jet printing [1], anti-icing [2,3], deicing [4], forensic identification [5] and solid actuating [6]. Over the past century, a lot of efforts have been spent on understanding the characteristics and underlying mechanisms of droplet impacting on solid surfaces [7-9]. It is now recognized that different phenomena may occur depending on the size, ingredient, physical properties, and impact velocity of droplets, as well as the wettability gradient, textured structure, and inclination of surfaces [10-13]. Deposition, sliding or rolling, partial or complete rebound, corona or prompt splash, and disintegrate are several possible scenarios [14-16]. For the most commonly studied rebound cases, two parameters are predominant, i.e., the bouncing height of droplet and contact time between droplet and surface.

Bouncing height is of great significance in engineering applications, where droplets are expected to rebound high enough in order to facilitate collection and discharge. Note that for tiny droplets, it is inertia rather than gravity that dominates impact dynamics [8]. As the effect of ambient gases is generally negligible [14], the bouncing height over a period of time virtually represents the bouncing velocity of droplets. The ratio of bouncing velocity to the impact velocity, i.e. the restitution coefficient, is commonly used to evaluate the degree of droplet energy dissipation during impact process.

Contact time is another focus in droplet impact, as it determines how much mass, momentum, and energy are transferred between droplets and surfaces [17]. Reducing contact time signifies a promotion in self-cleaning ability of surfaces, a delay or even

an inhibition of frosting and icing, as well as a decrease of energy loss. For many natural superhydrophobic surfaces (SHSs) such as lotus leaves, their water-repellent properties, hence the low contact time, mainly benefit from the multilevel structures on them [18]. In this context, modifying surface structures is a promising method to reduce contact time between droplets and surfaces.

Generally, the hydrodynamics of impacting droplets are assumed to be axisymmetric and the contact time is bounded below [19]. To break through the so-called Rayleigh limit, Bird et al. [20] introduced an asymmetric recoil of droplets by adding a macroscale texture to the surface, reducing the contact time by 37% and succeeding below the Rayleigh limit. Liu et al. [21] found that SHSs decorated with millimeter-scale tapered post arrays could trigger an abnormal bounce phenomenon where the droplets bounced off like a pancake directly after they reached the maximum expansion, decreasing the contact time by more than 50%. Lin et al. [22] used lattice Boltzmann method (LBM) to simulate the dynamics of droplets impacting on SHSs with large rectangular ridges. They concluded that non-axisymmetric spreading/retraction dynamics induced by ridges could largely decrease the contact time. Gauthier et al. [23] studied large droplets impacting on a small wire, while Liu et al. [24] studied the impact of small droplets on semi-cylindrical ridges with large curvature radius, both claiming an evident reduction in contact time. Andrew et al. [25] further proposed that the total contact time could be minimized when the obstacle diameter was close to that of the droplets, which is consistent with the experimental results by Guo et al. [26].

Recently there is increasing interest in understanding nanodroplet dynamics, and show many unique characteristics comparing to the macroscale counterpart have been

revealed [27,28]. Molecular dynamics (MD) is a computational tool that has been successfully applied to study the impact process of nanodroplets. For instance, Koplik et al. [14] employed MD to study the impact of nanodroplets of Lennard-Jones liquids, and observed various phenomena including stick, bounce, splash, and disintegrate, depending on the initial velocity and composition of droplets. Koishi et al. [29] and Gao et al. [30] used MD to study the bouncing performance of nanodroplets on columnar array structures, with a focus to develop the theories and models on the spreading dynamics and energy transformation, without the consideration of the contact time. Li et al. [31] investigated the effect of nanoridges on reducing liquid-solid contact time. It should be noted that they defined the droplets detaching point from the flat substrate rather than the nanoridge peak. Such a definition is reasonable for macro droplets, but becomes problematic at the nanoscale. as a dramatic energy transformation process should have been performed before touching the flat substrate. The contact time between nanodroplets and nanoridges usually accounts for a large proportion in the overall contact process.

Clearly the effect of nanostructures on the nanodroplets impact has not been well understood. To probe the physical mechanism of droplet impact, we perform a MD study in this work to reveal some interesting features of water nanodroplets impacting on SHSs decorated with different triangular nanoridges. Our results demonstrate that the introduction of nanoridges significantly promotes the bouncing performance of nanodroplets in terms of the bounce domain, redefined contact time, and the bouncing height, which is of high importance in designing nanostructured surfaces for targeted applications. .

Simulation Model and Method

We employ molecular dynamics (MD) to simulate the whole impact process of nanodroplets.. Owning to the rapid development of computational facilities, MD is becoming a powerful tool to probe complex dynamics of nanodroplets. s [32]. All our MD simulations are performed using the large-scale atomic/molecular massively parallel simulator (LAMMPS) [33], which is open source and has been successfully applied in many fields including physics, chemistry, , materials and engineering.

In this study, we construct 5 different triangular ridges and place them in the center of the top surface of a 54.0 nm × 27.0 nm × 0.74 nm plate. Physical dimensions of these ridges are displayed in Table 1. Nanodroplets of 4 different sizes, i.e. 64.4 Å, 81.2 Å, 102.5 Å, and 117.4 Å in diameter, corresponding to 4667, 9359, 18820, and 28288 water molecules, respectively, are put right above the nanoridge. The initial system and a partial enlarged view to the nanodroplet and nanoridge are schematically shown in Figure 1(a) and (b).

Table 1. Physical dimensions of nanoridges

Ridges		Height(Å)	Width(Å)	Vertex angle	Mark
Shapes	Sharp	32.48	9.64	33.06°	S
	Medium	32.48	14.46	48.00°	M
	Dull	32.48	28.92	83.36°	D
Sizes	Tiny	16.24	7.23	48.00°	T
	Medium	32.48	14.46	48.00°	M
	Big	48.72	21.69	48.00°	B

Table 2. Parameters of TIP4P/2005 model [34]

ϵ(kcal/mol)	σ (Å)	q_O(e)	q_H(e)	q_M(e)	r_{OM}(Å)	r_{OH}(Å)	θ_{HOH}(deg)
0.1852	3.1589	0	0.5564	-1.1128	0.1546	0.9572	104.52

The TIP4P/2005 model, which is a rigid planar model consisting of a Lennard-Jones potential site in the oxygen atom, three charged sites in a virtual *M* site and two

hydrogen atoms, is employed to simulate droplets. Pair potential between any two water molecules *i* and *j* is represented by a van-der-Waals term and a Coulomb term, namely $U_{ij} = 4\epsilon\left[\left(\frac{\sigma}{r_{OO}}\right)^{12} - \left(\frac{\sigma}{r_{OO}}\right)^{6}\right] + \frac{1}{4\pi\varepsilon_0}\sum_{a,b}\frac{q_a q_b}{r_{ab}}$, where r_{OO} is the distance between oxygen sites of two molecules, ε_0 is the vacuum permittivity, and *a* and *b* stand for the charged sites of molecules *i* and *j,* respectively [34]. The values of other TIP4P/2005 parameters are given in Table 2. Solid plates and nanoridges are composed of copper-like atoms, and a 12-6 Lennard-Jones potential is implemented on them with parameters $\sigma_{solid} = 2.616\,\text{Å}$ and $\epsilon_{solid} = 4.72\text{kcal/mol}$ [35]. Interactions between solid and droplet molecules are implemented by the Lennard-Jones potential with parameters determined by Lorentz-Berthelot mixing rules, i.e. $\sigma_{s,d} = (\sigma_{solid} + \sigma_O)/2$ and $\epsilon_{s,d} = k\sqrt{\epsilon_{solid}\epsilon_O}$, where *k* is a factor used for tuning the interaction strength [36,37]. Here we set *k*=0.05 to simulate a SHS and the corresponding equilibrium contact angle is around 152°~158°, determined by fitting the liquid-gas interface to an ellipse [38,39], as demonstrate in Figure 1(c).

Based on the preceding potentials and parameters, the forces between molecules can be determined, and the coordinates and velocities of molecules are updated by the Verlet integration method [40] with a time step of 1 fs. Each droplet has experienced sufficient relaxation in Nose-Hoover thermostat until its potential energy reaches a stable minimum. Then a macro downward velocity from 0.1 Å/ps to 14 Å/ps is exerted on the droplets, resulting in a vertical impact on nanoridges. The whole system (initially 298K) is simulated in the microcanonical ensemble during a sufficient simulation of 0.3 million steps.

It should be noted that the definition of contact time at the nanoscale relies on the configuration of surfaces (see details in Section 1 of Supplemental Materials), where

the ridge part should be considered. If the number of oxygen atoms in a near-wall layer is no more than N, where $N = 0.5\sqrt[3]{N_{O,total}}$, with $N_{O,total}$ the total number of oxygen atoms in nanodroplet, the droplet is considered to have detached from the surface. The thickness of contact layer is set as 4.1824 Å after a comprehensive parametric study, as shown in Figure 1(b). To make it more precise, all the time steps where the above criterion is satisfied are summed up, instead of merely calculating the interval between the first and last contact moment. On the other hand, the bouncing height of each droplet in this article is obtained from the displacement of its centroid during the time interval of 5τ after the maximum expansion. This time interval is far beyond the contact time of each droplet ($1.5\sim3.5\tau$ according to our simulation), and thus all these droplets have been sufficiently away from the surface when we obtain the data for their bouncing heights.

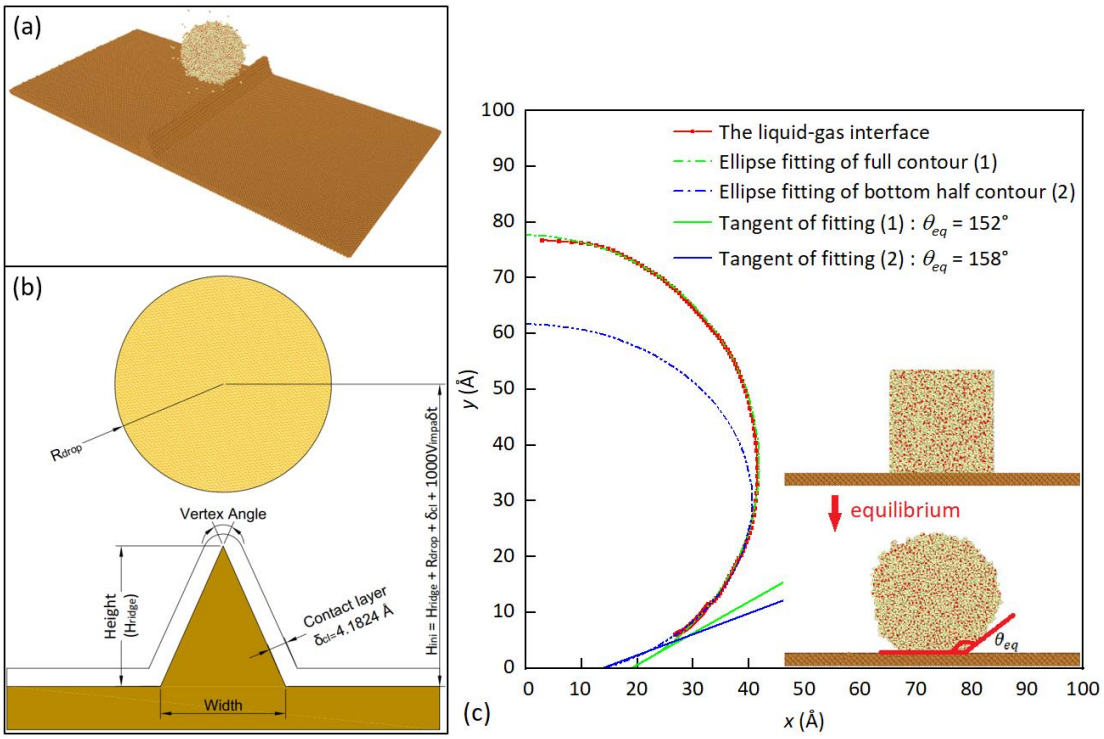

Figure 1. (a) A snapshot of the initial simulation system from perspective view. The orange-red, light-yellow and brown particles represent oxygen, hydrogen, and solid atoms, respectively. (b) A partial enlarged schematic diagram of nanodroplet and nanoridge from the front view. The initial

height of nanodroplet centroid to the substrate is $H_{ini} = H_{ridge} + R_{drop} + \delta_{cl} + 1000V_{impa}\delta t$, where V_{impa} is the impact velocity of nanodroplet, δ_{cl} is the thickness of contact layer, and δt signifies the time step of simulation. (c) Given the strength of interaction between droplet and surface, the equilibrium contact angle is measured around 152°~158° by fitting the whole or the bottom half liquid-gas interface to an ellipse.

For the sake of clarity, the dimensionless time, height, and velocity used below are normalized as $t^* = t/\tau$, $h^* = h/R$, and $v^* = v/v_r$, respectively, where $\tau = \sqrt{\rho R^3/\gamma}$ is the reference time scale corresponding to the capillary oscillation period of a perturbed inviscid droplet [41], R is droplet radius, and $v_r = \sqrt{\gamma/\rho R}$ is known as the capillary-inertia velocity (ρ and γ are the mass density and surface tension of nanodroplet) [42]. The weber number is defined as $We = (\rho \cdot 2R \cdot v^2)/\gamma$, which is the ratio of the inertia force to the capillary force.

Results and Discussions

1. Bounce performance of nanodroplets impacting on ridge-decorated surfaces.

We first compare the characteristics of nanodroplets impacting on ridge-decorated surfaces with those impacting on a flat SHS. Several typical snapshots are shown in Figure 2. It can be seen that droplets rebound from the flat surface only under a moderate impact velocity, e.g. 7 Å/ps in Figure 2(b). Otherwise they either vibrate back and forth and eventually settle on the surface, e.g. 4 Å/ps in Figure 2(a), or directly break up and eject lots of tiny pieces, e.g. 12 Å/ps in Figure 2(c). On the contrary, a nanoridge makes droplets with lower or higher impact velocities completely bounce off rather than deposit or splash, as shown in the last column of Figure 2. Given that in many practical engineering applications, a large number of droplets are expected to be collected and removed more effectively, this promotion can be significant, especially in nanoscale situations where the bounce domain of droplets impacting on flat surfaces

is quite narrow.

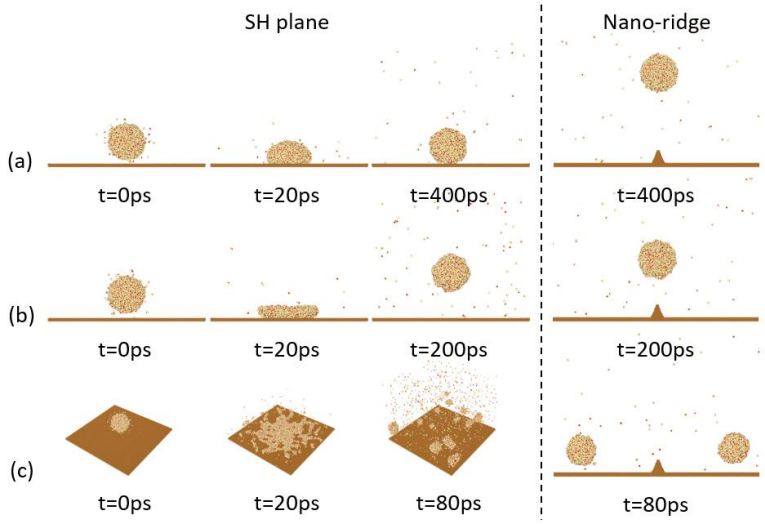

Figure 2. Snapshots of nanodroplets (D=81.2 Å) impacting on a flat SHS (the left three columns) and ridge-decorated SHS (the last column). (a) Droplet with impact velocity of 4 Å/ps adheres to the SH plane while rebounds from the ridged surface. (b) Droplet with impact velocity of 7 Å/ps rebounds from the SH plane as well as the ridged surface. (c) Droplet with impact velocity of 12 Å/ps splashes on SH plane but rebounds from the ridged surface.

To further quantify this phenomenon, we study nanodroplets (D=81.2 Å) with different velocities impacting on a variety of surfaces. It can be seen from Figure 3 that no matter what the shapes and sizes of nanoridges are, the bounce domains of ridge cases are always much wider than the plane cases. On the one hand, the nanoridges lower the upper velocity limit of deposition. When impacting on flat surfaces, because of their small size, nanodroplets require a tremendous velocity to reach the same magnitude of Weber number as macroscopic droplets to bounce off, and this value is 4~5 Å/ps according to our simulations. Moreover, when we tentatively use another flat surface with less hydrophobicity ($k = 0.08$, $\theta_{eq} = 124°\sim129°$), this bouncing threshold even goes up to 9 Å/ps, which is consistent with previous MD results [29]. On the contrary, no deposition is observed on the ridge-decorated surfaces even when the impact velocity goes down to 0.1 Å/ps, and this can be qualitatively explained by

the viewpoint of energy conservation. During the impact of nanodroplet, the kinetic energy, surface energy, and viscous dissipation energy are approximately balanced [43]. If a nanodroplet falls slowly on a flat surface, its kinetic energy will be depleted in multiple vibrations. The introduction of nanoridges, however, could greatly deform the nanodroplet during impact, and thus storing more surface energy with less energy dissipating than the cases without nanoridges. The stored surface energy, representing as an upward resultant force due to the asymmetry of the surface tension of the upper and lower surfaces, provides a boost for droplet rebounding. Once moving upward, the droplet is more prone to leaving, since there are far fewer solid atoms to attract it in the ridge peak than that of the flat substrate. The differences between these two processes can be intuitively observed by the temporal evolution of droplet vertical speed in Supplemental Materials (Section 2).

On the other hand, the nanoridges also raise the lower velocity limit of splashing from 11~12 Å/ps to 12~14 Å/ps, as shown in Figure 3. This is because the droplets are inclined to be split by nanoridges into two similar parts rather than disintegrate into pieces directly. The dimensionless velocity of two child-droplets reduces to about 89% of the initial velocity of their mother-droplet. Consequently, both child-droplets are down below the splashing threshold, and hence are capable of retracting and rebounding individually with an intact morphology.

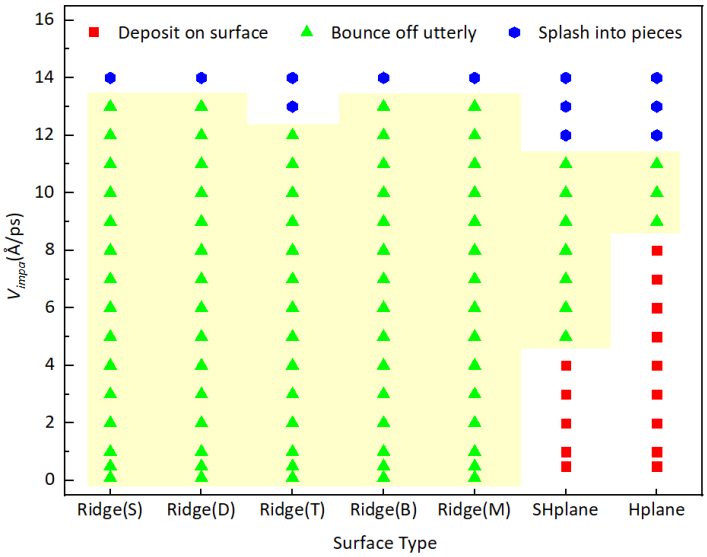

Figure 3. Dynamic behaviors of nanodroplets (D=81.2 Å) after impacting on surfaces decorated with a sharp, dull, tiny, big, and medium ridge, or on superhydrophobic (k=0.05) and hydrophobic (k=0.08) surface without any nanotextures. The physical dimensions of different ridges are given in Table 1. The bounce domains are displayed with pale yellow background, which refer to the impact velocity ranges where nanodroplets are able to bounce off the surface with a relatively intact morphology.

Besides the enlarged bounce domain, we further find that the bouncing properties are also enhanced due to the introduction of nanoridges. As shown in Figure 4(a) and (b), the nanoridges bring a shorter contact time and a larger bouncing height in most cases. When droplets impact with a moderate velocity, e.g. 5 Å/ps, the contact time is reduced by up to 40% and the bouncing height increases up to 300% owing to the nanoridges, while these promotions diminish as the impact velocity increases. For those nanodroplets with extremely high impact velocities, the reduction in contact time brought by nanoridges (around 20%) seems less noteworthy, because the contact time between nanodroplets and flat surfaces is already small enough; the nanoridges even bring a negative gain in bouncing height due to the split of nanodroplets, but it should be noted that the positive range $V_{impa} < 8\text{Å/ps}$ (i.e. $We < 72$) has covered most of the rebounding situations in engineering applications.

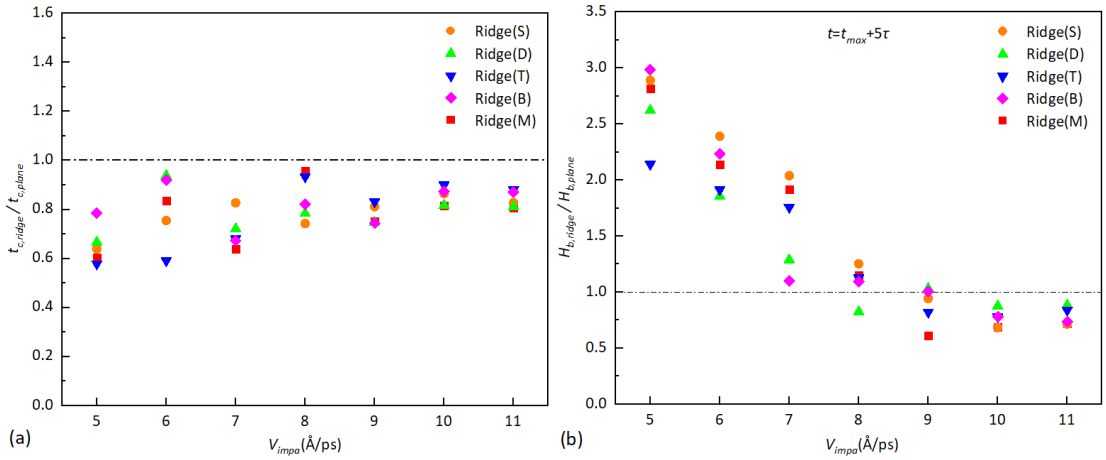

Figure 4. (a) The ratio of two contact times under different impact velocities, where $t_{c,ridge}$ is the contact time between nanodroplets and ridge-decorated surfaces, while $t_{c,plane}$ is that between nanodroplets and flat SH plane. The droplet diameter is 81.2 Å. (b) The ratio of droplet bouncing heights under two circumstances as described above. The time interval 5τ corresponds to 152.3 ps.

2. Bounce mechanism of nanodroplets impacting on ridge-decorated surfaces.

In this section we aim to elucidate the bounce mechanism of nanodroplets impacting on ridge-decorated surfaces. To this end, we first simulate nanodroplets with a diameter of 81.2 Å impacting on the medium-sized nanoridge with different impact velocities to observe how they rebound from the nanoridged surface. According to the snapshots shown in Figure 5, we identify them as 5 different bounce modes: State 1, bounce on ridge; State 2, retract and bounce on substrate; State 3, two lobes coalesce aloft but recontact the ridge; State 4, two lobes coalesce aloft without recontacting the ridge; State 5, split into two child droplets.

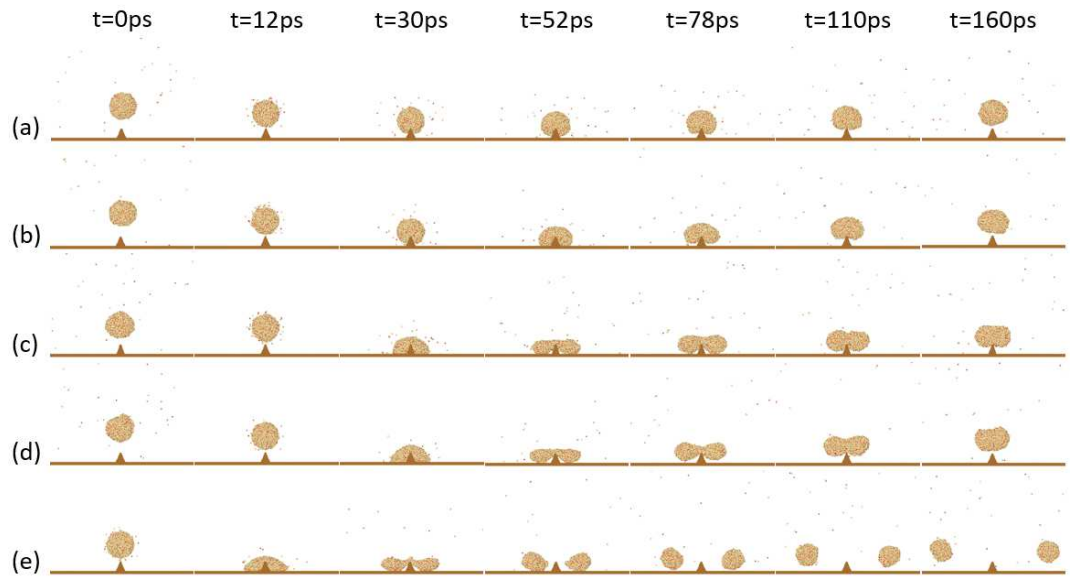

Figure 5. Snapshots of nanodroplets (D=81.2 Å) impacting on SHSs decorated with the medium-sized nanoridge. The impact velocities are (a) 2 Å/ps; (b) 4 Å/ps; (c) 6 Å/ps; (d) 7 Å/ps; (e) 8 Å/ps, corresponding to five different bounce modes.

We further simulate identical impact processes of nanodroplets with diameters of 64.4 Å, 102.5 Å, and 117.4 Å, and the dynamic behaviors of different bouncing droplets can always be classified into these typical bounce modes. The results shown in Figure 6(a) indicate that the impact velocity is the key factor in determining bounce modes, while the effect of droplet diameter is of less importance. If the impact velocity is normalized by the capillary-inertia velocity scale, i.e. $v_{impa}^{*} = v_{impa}/\sqrt{\gamma/\rho R}$, we find that these 5 states will emerge orderly as the v_{impa}^{*} increases, as shown in Figure 6(b). When impacting with a low velocity, i.e. $v_{impa}^{*} < 2.0$, nanodroplets will decelerate and rebound on nanoridge without touching the substrate (Figure 5(a), State 1). The larger the diameter is, the bigger inertia the droplet has, making it easier down to the substrate, and thus the shorter velocity range the State 1 occupies. If the impact velocity is moderate, i.e. $2.0 < v_{impa}^{*} < 4.0$, nanodroplets will expand and contract on the substrate, then climb along the nanoridge and eventually leave the surface (Figure 5(b), State 2). Most of published works are mainly focused on State 1 or 2 [20,22-26],

because the other bounce modes such as State 3 and 4 are inconspicuous and transient in macroscopic experiments and simulations.

However, for nanodroplets considered in this work, we find that when $4.0 < v_{impa}^{*} < 5.2$, the expanding droplet is gradually separated by the nanoridge into two lobes with a liquid bridge connecting them. Both lobes contract and bounce off the substrate individually, and then gather inward under the pulling of central liquid bridge. During this process of coalescence, two lobes come into contact with the nanoridge once again, and after releasing the excess surface energy, the coalesced droplet finally rebounds from the peak of the ridge (Figure 5(c), State 3). If the impact velocity increases to $5.2 < v_{impa}^{*} < 6.4$, the nanodroplet will expand more widely before retraction and the thickness of liquid bridge decreases because of the volume conservation. As a result, the retraction and rebound processes of both lobes accelerate, while the inward converging process slows down since the liquid bridge becomes weaker. Therefore, two lobes of droplet could have already bounced higher than the ridge peak during coalescence, avoiding the secondary contact with the nanoridge (Figure 5(d), State 4). If the impact velocity is particularly high, i.e. $v_{impa}^{*} > 6.4$, the liquid bridge would utterly break up during droplet retraction, resulting the split of nanodroplet. Then the split child droplets horizontally move away from the nanoridge, and rebound from the surface individually (Figure 5(e), State 5).

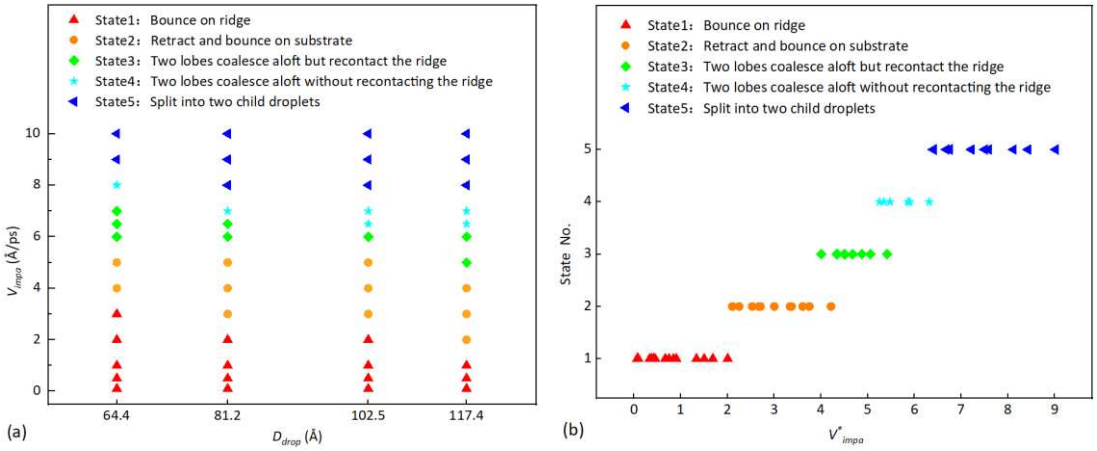

Figure 6. (a) Bounce mode of nanodroplets with four different diameters impacting on SHSs decorated with the medium-sized nanoridge. The impact velocities ranging from 0.1 Å/ps to 10 Å/ps are all within the bounce domain. (b) The dependence of bounce mode on the dimensionless impact velocity v^*_{impa}. The ordinates denote the mark numbers of bounce modes.

According to our simulation results, the contact time between nanodroplets and ridge-decorated surfaces do not present a simple step-like variation as the impact velocity increases, as shown in Figure 7. This distinction with the published work [31] may attribute to the different definition of contact time, and this kind of definition at nano scale can significantly affect the conclusions[37]. At first glance, the variation of dimensionless contact time with the impact velocity seems a little bit complicated. However, for each specific bounce mode, there is a general trend in contact time variation, and a simplified trendline is displayed in the inset of Figure 7.

Specifically, in the impact cases of State 1, we find that the upward resultant force on nanodroplets exerted by the nanoridge first significantly increases and then remains almost constant as the droplet falling (Force computation details are given in Section 3 of Supplemental Materials). This trend essentially accords with the variation of contact time in State 1 that first decreases and then increases with the impact velocity. Because when the velocity first starts growing, the rapid rise of upward force will stop the droplet more quickly, but then it takes longer to counteract this growing impact velocity

as the upward force becomes stagnant. Next, a reduction in contact time appears in State 2, and this does not contradict previous results claiming a nearly constant [31], because apart from the expansion and retraction process, we also add up the elapsed time of droplets lifting-up along the nanoridge. Apparently, a larger bouncing velocity helps decrease this climbing time, which is especially evident for smaller droplets. Then, the contact time shows a sharp increase in State 3 due to the secondary contact between droplet and nanoridge, while it falls back in State 4 as expected. The contact time in State 5 changes with a downward trend, and it is less than most of the non-split cases except for State 4. The derivations and explanations for these two phenomena are presented in Supplemental Materials (Section 4).

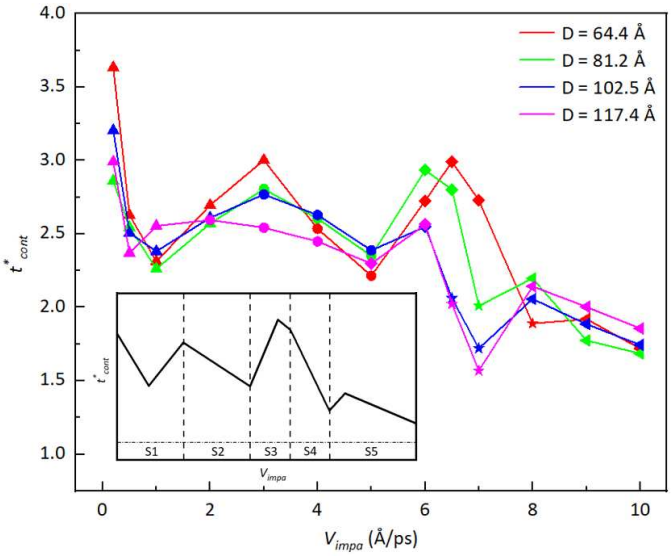

Figure 7. Variation of dimensionless contact time with the impact velocity of nanodroplets with four different diameters. The change laws of contact time for each bounce mode are simplified in the inset. The different symbols in each curve represent the corresponding bounce modes at certain impact velocity, specifically, the upper triangular, circle, diamond, star, and left triangular correspond to State 1~5 respectively.

On the other hand, the variation law of the bouncing height is much simpler than the contact time, as shown in Figure 8(a). There is a trend that the dimensionless bouncing height increases with the impact velocity, but with two small exceptions.

Generally, the bouncing velocity and hence the bouncing height during a certain period of time are positively related to the impact velocity. However, two reasons make the droplet bouncing velocity in State 4 smaller than that in State 3. First, two lobes of droplet in State 4 coalesce aloft and symmetrically, and hence with fewer repulsion and reaction forces exerted by the solid surface. Besides, the coalescing lobes in State 3 cling to the nanoridge that can help redirect a part of the horizontal inward velocity into the vertical upward direction [44]. Another exception appears at the outset of State 5 that the bouncing height decreases drastically owing to the split of droplet. The initial kinetic energy of droplet mainly transfers into the interfacial energy due to the newly formed surfaces of two child droplets, as well as the transverse kinetic energy of their horizontal motion. However, as the impact velocity keeps increasing, the bouncing height rapidly upswings.

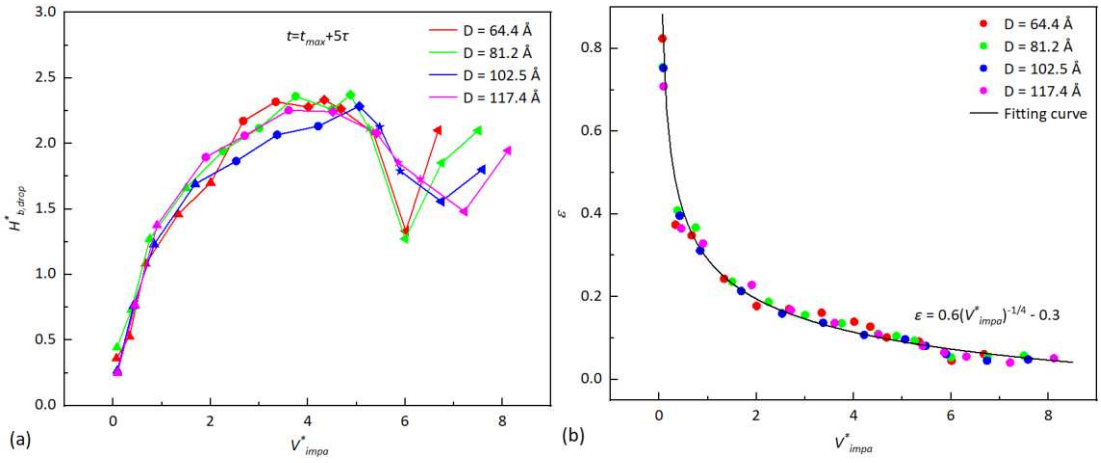

Figure 8. (a) Variation of the dimensionless bouncing height with the dimensionless impact velocity. The time interval 5τ corresponds to 107.6 ps, 152.3 ps, 216.0 ps, and 264.7 ps for the four diameters of nanodroplets. The upper triangular, circle, diamond, star, and left triangular represent State 1~5, respectively. (b) The velocity restitution coefficient of nanodroplets with four different diameters, fitted as a power function of the dimensionless impact velocity.

Although the absolute bouncing velocity monotonously increases with impact velocity in most cases, the velocity restitution coefficient presents an utterly opposite tendency, as shown in Figure 8(b). Our simulation results demonstrate that the

restitution coefficient can be fitted as a power function of the dimensionless impact velocity, i.e. $\varepsilon = 0.6(v_{impa}^{*})^{0.25} - 0.3$, and this relationship is independent of droplet diameter. It can be concluded that there is a vast viscous dissipation during high-speed impacts, which virtually impedes the pursuits for short contact time and large bouncing height through arbitrarily increasing the impact velocity, and hence it would be significant to take advantage of the aforementioned bounce mechanism.

3. The effect of ridge configuration on the droplet bounce performance.

In the following we study the effect of ridge configuration on the droplet bounce performance. To this end, we simulate nanodroplets with a constant diameter of 81.2 Å impacting on SHSs decorated with different nanoridges. As defined in Table 1, three kinds of the nanoridges keep the same height but with sharp, medium, or dull vertex angles, while the other three keep an identical vertex angle but with tiny, medium, or big dimensions. As shown in Figure 9(a), five bounce modes can be clearly identified for the former three cases (medium dimension, different vertex angles), and they will emerge orderly as the impact velocity increases, although there is a little bit difference in the velocity range of each state for different cases.

On the other hand, this difference is significantly amplified among the latter three cases (medium vertex angle, different sizes), with some of the bounce states even vanishing, as shown in Figure 9(b). For instance, when impacting on tiny ridges whose height is equivalent to 1/5 of the droplet diameter, the nanodroplet would always wrap around the tiny ridge during expansion and retraction, unless it rebounds on the nanoridge or splits into child-droplets. As a result, State 2 replaces State 3 and 4, and hence covers most of the velocity range. But it should be noted that even such a tiny

ridge can greatly improve the droplet bounce performance as presented before. On the contrary, the ridges with bigger sizes are able to buffer higher impact velocities before the droplets touch the substrate, manifesting as a larger range of State 1. Then the droplets will be divided into two lobes more separately than the smaller ridge cases, which means the State 2 tends to be replaced by State 3 and 4, with the State 5 emerging afterwards.

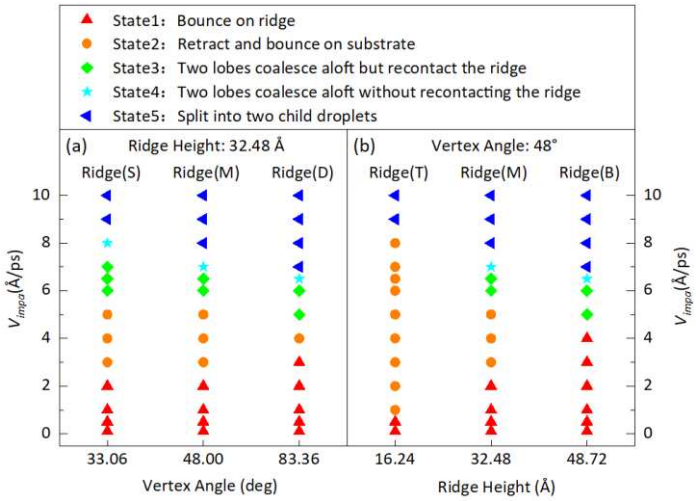

Figure 9. Bounce mode of nanodroplets (D=81.2 Å) impacting on SHSs decorated with nanoridges of different shapes (a) and sizes (b) as defined in Table 1.

The variations of nanodroplet contact time on different nanoridges are not perfectly in accordance with the medium ridge cases that have been discussed in last section, as shown in Figure 10. The reason for this is that the variation laws of contact time are based on the bounce modes of nanodroplets, and these bounce modes could change and even vanish depending on the different ridge configurations. For instance, all the five bounce modes exist in the sharp ridge cases, and hence its variation trend of contact time remains semblable with that of the medium ridge cases. On the contrary, the contact time in dull and big ridge cases present no downward trend inside the medium impact velocity range, mainly because of the transience or the absence of State 2. When the nanoridge is tiny, contact time changes with a small amplitude, akin to the

phenomenon of droplets impacting on flat planes. But note that for the remaining bounce states in each ridge configuration cases, the contact time still retains the variation characteristics as previously enunciated.

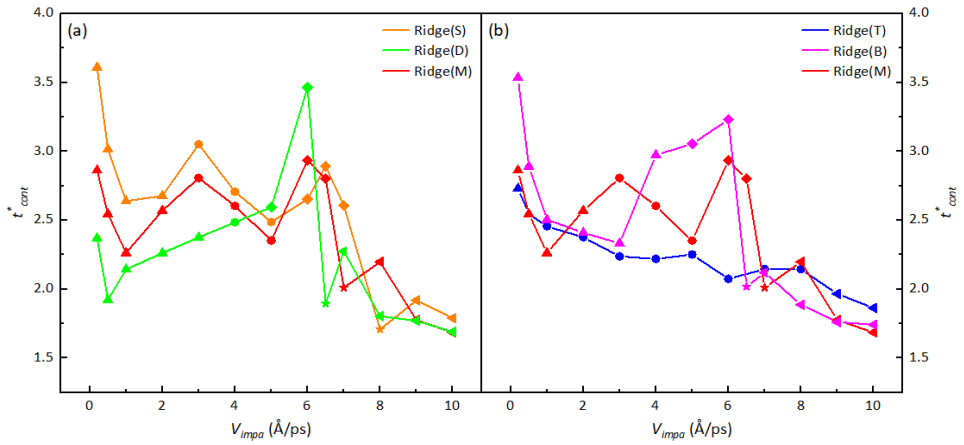

Figure 10. Variation of dimensionless contact time with the impact velocity of nanodroplets (D=81.2 Å). The nanoridges are of different shapes (a) and sizes (b) as defined in Table 1. The upper triangular, circle, diamond, star, and left triangular represent State 1~5, respectively.

On the other hand, the variations of nanodroplet bouncing height on different nanoridges are in complete conformity to the medium ridge cases, as shown in Figure 11(a). Since the dimensionless bouncing height increases with the impact velocity at State 1, 2, and 3, and then decreases at State 4 as well as the outset of State 5, this kind of state degeneracy prompts that the transience or absence of one or two states may not change the general trend of bouncing height. At last, as shown in Figure 11(b), the expression $\varepsilon = 0.6(v^*_{impa})^{0.25} - 0.3$ is still capable of describing the relationship between velocity restitution coefficient and the dimensionless impact velocity of nanodroplets, regardless of the shape and size of nanoridges.

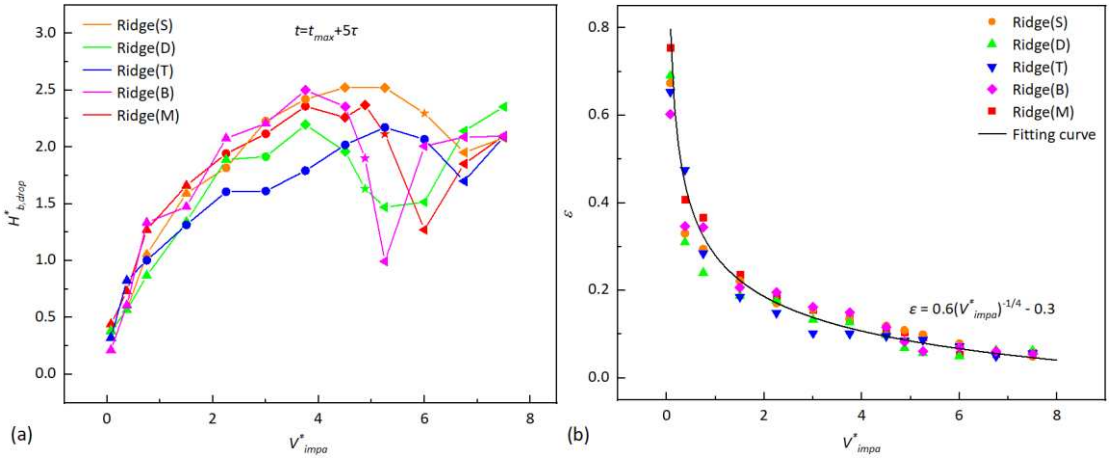

Figure 11. (a) Variation of the dimensionless bouncing height with the dimensionless impact velocity of nanodroplets (D=81.2 Å) on different ridge-decorated surfaces. The time interval 5τ corresponds to 152.3 ps. (b) The velocity restitution coefficient of nanodroplet (D=81.2 Å) on different ridge-decorated surfaces, fitted as a power function of the dimensionless impact velocity.

Conclusions

We performed molecular dynamics (MD) simulations to investigate water nanodroplets impacting on superhydrophobic surfaces decorated with different shapes and sizes of triangular nanoridges. Main conclusions are as follows:

(1) By introducing a nanoridge to the superhydrophobic surfaces, the bounce domain of impacting nanodroplets enlarges from 5~11 Å/ps to 0.1~13 Å/ps, empowering droplets with lower or higher impact velocities to completely bounce off rather than adhere to the surface or splash into pieces.

(2) The contact time is reduced by up to 40% and the bouncing height increases up to 300% due to the effect of nanoridge. Although these promotions dwindle away as the impact velocity increases, the positive range (We<72) generally covers the vast majority of rebounding cases in engineering applications.

(3) The bounce modes of impacting droplets on ridge-decorated surfaces can be classified into five distinct states, i.e., bounce on ridge, retract and bounce on substrate, two lobes coalesce aloft but recontact the ridge, two lobes coalesce aloft

without recontacting the ridge and split into two child droplets, emerging in sequence with the increase of dimensionless impact velocity. The variation laws of contact time and bouncing height of droplets under different diameters and impact velocities are determined by the characteristics of each states.

(4) Ridge configurations, especially the ridge size, can alter the bounce modes of nanodroplets, and thus the variation laws of contact time and bouncing height will change accordingly.

(5) The variation of velocity restitution coefficient can be always fitted as a power function of the dimensionless impact velocity, i.e. $\varepsilon = 0.6(v_{impa}^{*})^{0.25} - 0.3$, regardless of the different characteristics of nanodroplets and the nanoridges.

Supplemental Materials

The definition of contact time; Nanodroplets impacting on surfaces under low impact velocities; Force computation in the cases of State 1; Derivation and explanations for the contact time variation in State 5.

Acknowledgments

This work was supported by National Natural Science Foundation of China (Grant No. 11772034) and Beijing Natural Science Foundation (Grant No. 3204048).

Conflict of interest

We declare no conflict of interest.

References

[1] P. Galliker, J. Schneider, H. Eghlidi, S. Kress, V. Sandoghdar, and D. Poulikakos, Direct printing of nanostructures by electrostatic autofocussing of ink nanodroplets, Nat. Commun. **3**, 890 (2012).

[2] T. Maitra, C. Antonini, M. K. Tiwari, A. Mularczyk, Z. Imeri, P. Schoch, and D.

Poulikakos, Supercooled Water Drops Impacting Superhydrophobic Textures, Langmuir **30**, 10855 (2014).
[3] L. Mishchenko, B. Hatton, V. Bahadur, J. A. Taylor, T. Krupenkin, and J. Aizenberg, Design of Ice-free Nanostructured Surfaces Based on Repulsion of Impacting Water Droplets, ACS Nano **4**, 7699 (2010).
[4] F. Chu, X. Wu, and L. Wang, Dynamic Melting of Freezing Droplets on Ultraslippery Superhydrophobic Surfaces, ACS Appl. Mater. Interfaces **9**, 8420 (2017).
[5] D. Attinger, C. Moore, A. Donaldson, A. Jafari, and H. A. Stone, Fluid dynamics topics in bloodstain pattern analysis: Comparative review and research opportunities, Forensic Sci. Int. **231**, 375 (2013).
[6] H. Li, W. Fang, Y. Li, Q. Yang, M. Li, Q. Li, X. Q. Feng, and Y. Song, Spontaneous droplets gyrating via asymmetric self-splitting on heterogeneous surfaces, Nat. Commun. **10**, 950 (2019).
[7] A. L. Yarin, Drop impact dynamics: Splashing, spreading, receding, bouncing, Annu. Rev. Fluid. Mech **38**, 159 (2006).
[8] C. Josserand and S. T. Thoroddsen, Drop Impact on a Solid Surface, Annu. Rev. Fluid. Mech **48**, 365 (2016).
[9] D. Khojasteh, M. Kazerooni, S. Salarian, and R. Kamali, Droplet impact on superhydrophobic surfaces: A review of recent developments, J. Ind. Eng. Chem. **42**, 1 (2016).
[10] M. Reyssat, Pépin, F. Marty, Chen, and D. Quéré, Bouncing transitions on microtextured materials, Europhys. Lett. **74**, 306 (2007).
[11] R. Rioboo, C. Tropea, and M. Marengo, Outcomes from a drop impact on solid surfaces, Atomization Sprays **11**, 155 (2001).
[12] C. Antonini, F. Villa, and M. Marengo, Oblique impacts of water drops onto hydrophobic and superhydrophobic surfaces: outcomes, timing, and rebound maps, Exp. Fluids **55**, 1713 (2014).
[13] D. Vadillo, J. Hinch, I. Hutchings, and K. Yokoi, Numerical studies of the influence of the dynamic contact angle on a droplet impacting on a dry surface, Phys. Fluids **21**, 72102 (2009).
[14] J. Koplik and R. Zhang, Nanodrop impact on solid surfaces, Phys. Fluids **25**, 022003 (2013).
[15] H. Almohammadi and A. Amirfazli, Asymmetric Spreading of a Drop upon Impact onto a Surface, Langmuir **33**, 5957 (2017).
[16] J. Qu, Y. Yang, S. Yang, D. Hu, and H. Qiu, Droplet impingement on nano-textured superhydrophobic surface: Experimental and numerical study, Appl. Surf. Sci. **491**, 160

(2019).
[17] R. B. Bird, W. E. Stewart, and E. N. Lightfoot, *Transport Phenomena* (John Wiley & Sons, New York, 2007).
[18] T.-S. Wong, S. H. Kang, S. K. Y. Tang, E. J. Smythe, B. D. Hatton, A. Grinthal, and J. Aizenberg, Bioinspired self-repairing slippery surfaces with pressure-stable omniphobicity, Nature **477**, 443 (2011).
[19] D. Richard, C. Clanet, and D. Quere, Surface phenomena - Contact time of a bouncing drop, Nature **417**, 811 (2002).
[20] J. C. Bird, R. Dhiman, H. M. Kwon, and K. K. Varanasi, Reducing the contact time of a bouncing drop, Nature **503**, 385 (2013).
[21] Y. H. Liu, G. Whyman, E. Bormashenko, C. L. Hao, and Z. K. Wang, Controlling drop bouncing using surfaces with gradient features, Appl. Phys. Lett. **107**, 051604 (2015).
[22] D.-J. Lin, L. Wang, X.-D. Wang, and W.-M. Yan, Reduction in the contact time of impacting droplets by decorating a rectangular ridge on superhydrophobic surfaces, Int. J. Heat Mass Transfer **132**, 1105 (2019).
[23] A. Gauthier, S. Symon, C. Clanet, and D. Quere, Water impacting on superhydrophobic macrotextures, Nat. Commun. **6**, 8001 (2015).
[24] Y. H. Liu, M. Andrew, J. Li, J. M. Yeomans, and Z. K. Wang, Symmetry breaking in drop bouncing on curved surfaces, Nat. Commun. **6**, 10034 (2015).
[25] M. Andrew, Y. Liu, and J. M. Yeomans, Variation of the Contact Time of Droplets Bouncing on Cylindrical Ridges with Ridge Size, Langmuir **33**, 7583 (2017).
[26] C. Guo, J. Sun, Y. Sun, M. Wang, and D. Zhao, Droplet impact on cross-scale cylindrical superhydrophobic surfaces, Appl. Phys. Lett. **112**, 263702 (2018).
[27] R. Bardia, Z. Liang, P. Keblinski, and M. Trujillo, Continuum and molecular-dynamics simulation of nanodroplet collisions, Phys. Rev. E **93**, 053104 (2016).
[28] R. Holyst, M. Litniewski, and D. Jakubczyk, Evaporation of liquid droplets of nano- and micro-meter size as a function of molecular mass and intermolecular interactions: experiments and molecular dynamics simulations, Soft Matter **13**, 5858 (2017).
[29] T. Koishi, K. Yasuoka, and X. C. Zeng, Molecular Dynamics Simulation of Water Nanodroplet Bounce Back from Flat and Nanopillared Surface, Langmuir **33**, 10184 (2017).
[30] S. Gao, Q. Liao, W. Liu, and Z. Liu, Nanodroplets Impact on Rough Surfaces: A Simulation and Theoretical Study, Langmuir **34**, 5910 (2018).
[31] T. Li, L. Zhang, Z. Wang, Y. Duan, J. Li, J. Wang, and H. Li, Bouncing dynamics

of liquid drops impact on ridge structure: an effective approach to reduce the contact time, Phys. Chem. Chem. Phys. **20**, 16493 (2018).
[32] D. C. Rapaport, *The Art of Molecular Dynamics Simulation* (Cambridge university press, Cambridge, 1995).
[33] S. Plimpton, Fast Parallel Algorithms for Short-Range Molecular Dynamics, J. Comput. Phys. **117**, 1 (1995).
[34] J. L. F. Abascala and C. Vega, A general purpose model for the condensed phases of water_TIP4P_2005, J. Chem. Phys. **123**, 234505 (2005).
[35] H. Heinz, R. A. Vaia, B. L. Farmer, and R. R. Naik, Accurate Simulation of Surfaces and Interfaces of Face-Centered Cubic Metals Using 12−6 and 9−6 Lennard-Jones Potentials, J. Phys. Chem. **112**, 17281 (2008).
[36] J. Zhang, M. K. Borg, K. Sefiane, and J. M. Reese, Wetting and evaporation of salt-water nanodroplets: A molecular dynamics investigation, Phys. Rev. E **92**, 052403 (2015).
[37] J. Zhang, P. F. Wang, M. K. Borg, J. M. Reese, and D. S. Wen, A critical assessment of the line tension determined by the modified Young's equation, Phys. Fluids **30**, 082003 (2018).
[38] K. Ritos, N. Dongari, M. K. Borg, Y. Zhang, and J. M. Reese, Dynamics of Nanoscale Droplets on Moving Surfaces, Langmuir **29**, 6936 (2013).
[39] J. Zhang, M. K. Borg, and J. M. Reese, Multiscale simulation of dynamic wetting, Int. J. Heat Mass Transfer **115**, 886 (2017).
[40] D. Levesque and L. Verlet, Molecular dynamics and time reversibility, J. Stat. Phys. **72**, 519 (1993).
[41] D. Bartolo, C. Josserand, and D. Bonn, Retraction dynamics of aqueous drops upon impact on non-wetting surfaces, J. Fluid Mech. **545**, 329 (2005).
[42] M. Stange, M. Dreyer, and H. Rath, Capillary driven flow in circular cylindrical tubes, Phys. Fluids **15**, 2587 (2003).
[43] J. Guo, S. Lin, B. Zhao, X. Deng, and L. Chen, Spreading of impinging droplets on nanostructured superhydrophobic surfaces, Appl. Phys. Lett. **113**, 071602 (2018).
[44] H. Vahabi, W. Wang, J. M. Mabry, and A. K. Kota, Coalescence-induced jumping of droplets on superomniphobic surfaces with macrotexture, Sci. Adv **4**, eaau3488 (2018).